Directional Cell Search for Millimeter Wave Cellular Systems

C. Nicolas Barati, S. Amir Hosseini, Sundeep Rangan, Pei Liu, Thanasis Korakis, Shivendra S. Panwar
Department of Electrical and Computer Engineering
NYU Polytechnic School of Engineering, Brooklyn, New York 11201
Email:{nicolas.barati,amirhs.hosseini,srangan}@nyu.edu, {pliu,korakis}@poly.edu, panwar@catt.poly.edu

***Abstract*—Millimeter wave (mmW) bands between 30 and 300 GHz are considered a promising candidate for next-generation cellular networks to relieve spectral congestion in conventional cellular frequencies. However, cellular communication at these frequencies will likely require highly directional transmissions to achieve suitable signal range. This reliance on directional beamforming complicates initial cell search since the mobile and base station must jointly search over a potentially large angular directional space to locate a suitable path to initiate communication. This paper proposes a directional cell search procedure where each base station periodically transmits synchronization signals in randomly varying directions. Detectors are derived for this synchronization signal based on a Generalized Likelihood Ratio Test (GLRT) for the case where (i) the mobile has only analog beamforming (where the mobile can "look" in only direction at a time) and (ii) digital beamforming where the mobile has access to digital samples from all antennas. Simulations under realistic parameters demonstrate that mobiles may not be able to achieve suitable detection performance with analog beamforming alone. In contrast, digital beamforming offers dramatically better performance. We argue that the additional power consumption cost of digital beamforming can be offset by using very low quantization rates with minimal performance loss, thus arguing that low-rate fully digital front-ends may be a better design choice for directional cell search.**

I. Introduction

Millimeter wave (mmW) systems between 30 and 300 GHz have attracted considerable recent attention for next-generation cellular networks [1]–[3]. The mmW bands offer orders of magnitude more spectrum than current cellular allocations – up to 200 times by some estimates. However, a key challenge in mmW cellular is the signal range. Due to Friis' Law [4], the high frequencies of mmW signals result in large isotropic path loss (the free-space path loss grows with the frequency squared). Fortunately, the small wavelengths of these signals also enable large number of antenna elements to be placed in the same physical antenna area thereby providing high beamforming gains that can theoretically more than compensate for the increase in isotropic path loss [5].

However, for cellular systems, the reliance on highly directional transmissions significantly complicates initial cell search. While current cellular systems such as 3GPP LTE [6] have considerable support for beamforming and multi-antenna technologies, the underlying design assumption is that initial network discovery can be conducted entirely with omni-directional transmissions or transmissions in fixed antenna patterns. LTE base stations, for example, generally do not apply beamforming when transmitting the synchronization and broadcast signals. Adaptive beamforming and user-specific directional transmissions are generally used only *after* the physical-layer access has been established.

In contrast, to overcome the high isotropic path loss, mmW systems will likely need to employ directional transmissions even in the cell search phase to find base stations and directions of transmissions to those base stations. Network discovery will thus have a fundamental added dimension of searching not present in current cellular systems: not only must base stations and mobiles detect one another, they must detect the spatial angles of transmission on which communication can be performed.

In this paper, we propose and analyze a simple directional cell search procedure where the base station periodically transmits a synchronization signal, but with randomly varying directions to scan the angular space. The synchronization signal is similar to the primary synchronization signal (PSS) channel used in LTE but with randomly varying transmission angles.

At the mobile receiver, a key challenge for detecting such a synchronization signal is that it is generally not possible from a power consumption perspective to obtain high rate digital samples from all antenna elements. Most proposed designs perform beamforming in analog (either in RF or IF) prior to the A/D conversion [7]–[10]. A key limitation for these architectures is that they permit the mobile to "look" in only one or a small number of directions at a time. To investigate the effect of this constraint we consider two detection scenarios: (i) *analog beamforming* where the mobile beamforms in a random angular direction in each PSS time slot; and (ii) *digital beamforming* where the mobile has access to digital samples from all the antenna elements.

We derive generalized likelihood ratio test (GLRT) detectors [11] for both the analog and digital beamforming cases, treating the unknown spatial direction and time-varying channel gains as unknown parameters. We show that for analog beamforming, the GLRT detection is equivalent to matched filter detection with non-coherent combining across multiple PSS time slots. For digital beamforming, the GLRT detector can be realized via a vector correlation across all the antennas followed by a maximal eigenvector that finds the optimal spatial direction. Both detectors are computationally easy to implement.

Both detectors are simulated under realistic system pa-

rameters. Interestingly, the simulations indicate that analog beamforming with GLRT detection is likely to be unable to detect base stations under practical design requirements for the overhead, search time and antenna dimensions. Specifically, we argue that a mobile should be able to detect a base station at any SNR such that, *if the optimal beamforming directions were known*, the mobile could obtain a reasonable target rate. When the mobile and base station have a very high-gain antennas, this target SNR may be very low. Our simulations consider the case of a reasonable cell edge rate target for mmW systems of 10 Mbps in a 1 GHz bandwidth and antenna gains of 30 dBi combined on the BS and mobile. In this case, we show that the corresponding target SNR is so low that correlation detection with analog beamforming cannot detect the PSS signals reliably.

However, we also show that digital beamforming offers dramatically better performance and can easily meet the target SNR requirements since it eliminates the searching in the receive direction. The main difficulty with digital beamforming is the high power consumption in the A/D conversion. We argue that digital beamforming with very low bit rate (say 2 to 3 bits per antenna) as proposed by [12], [13] may be able to achieve good detection performance with acceptable power consumption. We thus conclude that low-bit rate fully digital front-ends may be a superior design choice in the mmW range, at least for the purpose of cell search. Due to space considerations, some details in this paper are omitted: a full paper [14] contains all the derivations and more detailed discussions of the simulations.

II. Proposed Synchronization Signal Design

In the current LTE standard, each base station cell (called the evolved NodeB or eNB) periodically broadcast two signals: the Primary Synchronization Signal (PSS) and the Secondary Synchronization Signal (SSS). The mobiles (called the user equipment or UE) search for the cells by scanning various frequency bands for the presence of these signals. The mobiles first search for the PSS which provides a coarse estimate of the frame timing, frequency offset and receive power. To simplify the detection, only one of three PSS signals are transmitted. Once the PSS is detected, the UE can search for the SSS. Since the frame timing and frequency offset of the eNB are already determined at this point, the SSS can belong to a larger set of 168 waveforms. The index of the detected PSS and SSS waveforms together convey the eNB cell identity.

In this work, we focus on the PSS design for mmW systems since this is the channel that needs to be most significantly changed for mmW. We consider a PSS transmission scheme shown in Fig. 1. Similar to the LTE PSS, we assume the signal is transmitted periodically once every T_{per} seconds in a brief interval of length T_{sig}. We will call the short interval of length T_{sig} the *PSS time slot*, and the period between of length T_{per} between two PSS slots, the *PSS period*. The selection of T_{sig}, T_{per} and other parameters will be discussed below. However, while LTE base stations generally transmit the PSS omni-directionally or in a fixed direction, here we suppose that the base station randomly transmits the PSS signal in a different direction in each PSS time slot, thereby scanning the angular space.

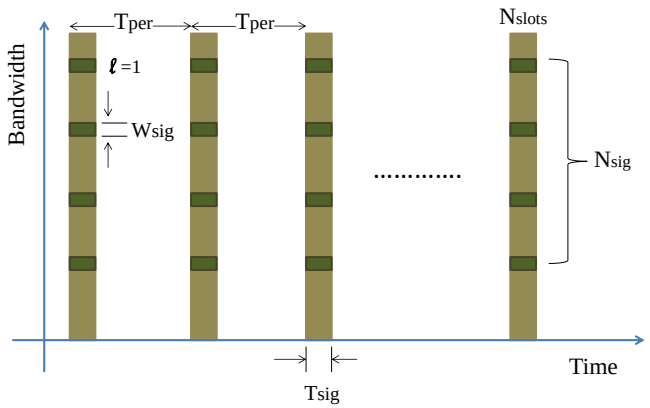

Fig. 1: Proposed PSS periodic transmission.

Also, to exploit the higher bandwidths, we assume that, in each PSS time slot, the PSS waveform be transmitted over N_{sig} PSS sub-signals. The use of multiple sub-signals can provide frequency diversity. In current LTE systems, the PSS signal is transmitted over a relatively narrowband of approximately of 930 kHz. Here, we will assume that each PSS sub-signal is narrowband, with some bandwidth W_{sig}.

III. PSS Detector

A. Signal Model

Consider the transmission of a PSS signal from a BS with N_{tx} antennas to a mobile with N_{rx} receive antennas. Index all the PSS sub-signals across all PSS time slots by ℓ. Then we can write the complex baseband waveform for the PSS transmission from the BS as

$$\mathbf{x}(t) = \sum_{\ell=-\infty}^{\infty} \mathbf{w}_{\ell}^{tx} p_{\ell}(t),$$

where $\mathbf{x}(t) \in \mathbb{C}^{N_{tx}}$ is the vector of complex signals to the N_{tx} antennas, $p_{\ell}(t)$ is the scalar PSS sub-signal waveform in the ℓ-th time-frequency slot and $\mathbf{w}_{\ell}^{tx}$ is the TX beamforming vector applied to the ℓ-th sub-signal.

For the purpose of the detector, we will make two key assumptions: First, we assume that the channel is flat in the time-frequency region around each PSS sub-signal. Thus, the channel can be described by a sequence of channel matrices $\mathbf{H}_{\ell} \in \mathbb{C}^{N_{rx} \times N_{tx}}$ representing the complex channel gain between the BS and mobile around the ℓ-th PSS sub-signal. Secondly, we will assume that the channel is rank one, which corresponds physically to a single path with no angular dispersion. In this case, the channel gain matrix can be written

$$\mathbf{H}_{\ell} = g_{\ell} \mathbf{u} \mathbf{v}^*,$$

where g_{ℓ} is the small-scale fading of the channel in the ℓ-th sub-signal and $\mathbf{u}$ and $\mathbf{v}$ are the RX and TX spatial signatures, which are determined by the large scale path directions and antenna patterns at the RX and TX. We assume that $\mathbf{u}$ and $\mathbf{v}$

do not change over the detection period – hence there is no dependence on ℓ.

Under these channel assumptions, the receiver will see a complex signal of the form,

$$\mathbf{y}(t) = \sum_{\ell=-\infty}^{\infty} \alpha_\ell \mathbf{u} p_\ell(t-\tau) + \mathbf{d}(t), \tag{1}$$

where $\mathbf{y}(t)$ is the vector of RX signals across the N_{rx} antennas, τ is the delay of the PSS signal, α_ℓ is the effective channel gain

$$\alpha_\ell = g_\ell \mathbf{v}^* \mathbf{w}_\ell^{tx}, \tag{2}$$

and $\mathbf{d}(t)$ is AWGN.

B. GLRT Detection with Digital RX Beamforming

The object of the mobile receiver is to determine, for each possible delay offset τ, whether a PSS signal is present at that delay or not. Since the PSS is periodic with period T_{per}, the receiver need only test delay hypotheses in the interval $\tau \in [0, T_{per}]$.

We first consider this PSS detection problem in the case when the mobile can perform digital RX beamforming. In this case, the mobile receiver has access to digital samples from each of the individual components of the vector $\mathbf{y}(t)$ in (1). We will assume that the detection is performed using N_{slot} PSS time slots of data which we index by $k = 1, \ldots, N_{slot}$. Note that there are $L = N_{sig} N_{slot}$ sub-signals in this period.

We can now pose the detection of the PSS signal as binary hypothesis problem: For each delay candidate τ, a PSS signal is either present with that delay (the H_1 hypothesis) or is not present (the H_0 hypothesis). Following (1), we will assume a signal model for the two hypotheses of the form

$$H_1: \ \mathbf{y}(t) = \sum_{\ell=-\infty}^{\infty} \alpha_\ell \mathbf{u} p_\ell(t-\tau) + \mathbf{d}(t), \tag{3a}$$

$$H_0: \ \mathbf{y}(t) = \mathbf{d}(t), \tag{3b}$$

where $\mathbf{d}(t)$ is complex white Gaussian noise with some power spectral density matrix $\nu \mathbf{I}$. Let $\boldsymbol{\theta}$ be the vector of all the unknown parameters,

$$\boldsymbol{\theta} = (\mathbf{u}, \nu, \alpha_1, \ldots, \alpha_L).$$

Due to the presence of these unknown parameters, we use a Generalized Likelihood Ratio Test (GLRT) to decide between the two hypotheses:

$$\Lambda(\tau) := \log \frac{\max_{\boldsymbol{\theta}} p(Y_\tau | H_1, \boldsymbol{\theta})}{\max_{\boldsymbol{\theta}} p(Y_\tau | H_0, \boldsymbol{\theta})} \underset{H_0}{\overset{H_1}{\gtrless}} t' \tag{4}$$

where t' is a threshold, Y_τ is the data $\mathbf{y}(t-\tau)$ in the N_{slot} PSS time slots and $p(Y_\tau | H_i, \boldsymbol{\theta})$ is the probability density of the received signal data Y_τ under the hypothesis H_0 or H_1 and parameters $\boldsymbol{\theta}$. The GLR $\Lambda(\tau)$ is the ratio of the likelihoods under the two hypotheses, maximized under the unknown parameters.

It is shown in the full paper [14] that the GLRT (4) can be evaluated via a simple correlation. Specifically, let $\mathbf{v}_\ell(\tau)$ be the normalized matched-filter detector for the ℓ-th subsignal,

$$\mathbf{v}_\ell(\tau) = \frac{1}{\|p_\ell\|} \int p_\ell^*(t) \mathbf{y}(t-\tau) dt, \quad \|p_\ell\|^2 := \int |p(t)|^2 dt. \tag{5}$$

Also, let $E(\tau)$ be the total received energy in the N_{slot} PSS time slots under the delay τ,

$$E(\tau) = \sum_{k=1}^{N_{slot}} \int_{I_k} \|\mathbf{y}(t-\tau)\|^2 dt, \tag{6}$$

where I_k is the interval for the k-th time slot. Then, it is shown that, for any threshold level t', there exists a threshold level t such that the GLRT in (4) is equivalent to a test of the form,

$$T(\tau) = \frac{\sigma_{max}^2(\mathbf{V}(\tau))}{E(\tau)} \underset{H_0}{\overset{H_1}{\gtrless}} t \tag{7}$$

where t is a threshold level, $\mathbf{V}(\tau) \in \mathbb{C}^{N_{rx} \times L}$ is the matrix

$$\mathbf{V}(\tau) := [\mathbf{v}_1(\tau), \cdots \mathbf{v}_L(\tau)], \tag{8}$$

and $\sigma_{max}(\mathbf{V}(\tau))$ is the largest singular value of the matrix. The detector has a natural interpretation: First, we perform a matched filter correlator for each sub-signal $p_\ell(t)$ on each of the vector $\mathbf{y}(t)$ yielding a a vector correlation output $\mathbf{v}_\ell(\tau)$. We then compute the max singular vector for the matrix $\mathbf{V}(\tau)$ which finds the energy in the most likely spatial direction across all the L sub-signals.

C. GLRT for Analog Beamforming

We next consider the hypothesis testing problem in the case when the mobile receiver can only perform beamforming in analog (either at RF or IF). In this case, for each PSS time slot k, the RX must select a receive beamforming vector $\mathbf{w}_k^{rx} \in \mathbb{C}^{N_{rx}}$ and then only observes the samples in this direction. If we let $z(t)$ be the scalar output from applying the beamforming vector $\mathbf{w}_k^{rx}$ to the received vector $\mathbf{y}(t)$, the signal model for the two hypotheses in (3) is transformed to

$$H_1: \ z(t) = \sum_{\ell=-\infty}^{\infty} \beta_\ell p_\ell(t-\tau) + d(t), \tag{9a}$$

$$H_0: \ z(t) = d(t), \tag{9b}$$

where the β_ℓ effective gain after TX and RX beamforming and $d(t)$ is complex white Gaussian noise with some PSD ν. From (2), the beamforming gain will be given by

$$\beta_\ell := g_\ell \mathbf{w}_k^{rx*} \mathbf{u} \mathbf{v}^* \mathbf{w}_k^{tx}, \tag{10}$$

for all sub-signals ℓ in the time slot k Here, we have assumed that both the TX and RX must apply the same beamforming gains for all sub-signals in the same PSS time slot. This requirement is necessary since, under analog beamforming, both the TX and RX can use only one beam direction at a time. The unknown parameters in the analog case can be described by the vector $\boldsymbol{\theta} = (\nu, \beta_1, \ldots, \beta_L)$.

Analogous to (4), we use a GLRT test of the form

$$\Lambda(\tau) := \log \frac{\max_{\boldsymbol{\theta}} p(Z_\tau | H_1, \boldsymbol{\theta})}{\max_{\boldsymbol{\theta}} p(Z_\tau | H_0, \boldsymbol{\theta})} \underset{H_0}{\overset{H_1}{\gtrless}} t' \tag{11}$$

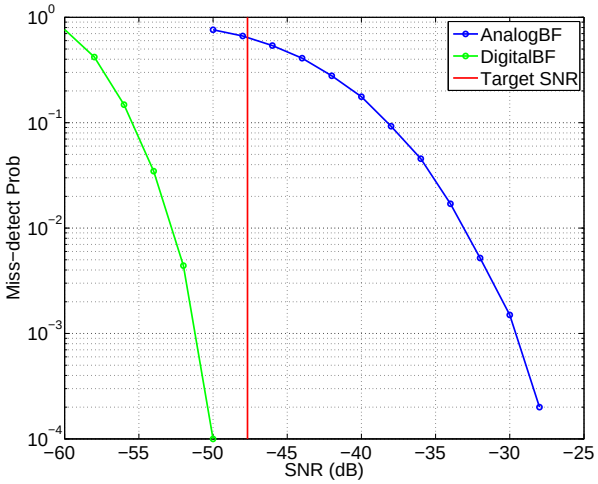

Fig. 2: Misdetection Probability vs. PSS SNR: Digital BF (green), Analog BF (blue), Target SNR for $R_{tgt} = 10$ Mbps (red)

where t' is a threshold level and Z_τ is the beamformed signal $\mathbf{z}(t-\tau)$ in the N_{slot} PSS time slots.

Similar to the digital case, this GLRT can be evaluated via a correlation. Let $v_\ell(\tau)$ be normalized correlation of $z(t)$ with the sub-signal $p_\ell(t)$,

$$v_\ell(\tau) = \frac{1}{\|p_\ell\|}\int p_\ell^*(t)z(t-\tau)dt, \quad \|p_\ell\|^2 := \int |p(t)|^2 dt. \tag{12}$$

It is shown in the full paper [14] that GLRT test (11) is equivalent to a test of the form

$$T(\tau) = \frac{\|\mathbf{v}(\tau)\|^2}{E(\tau)} \underset{H_0}{\overset{H_1}{\gtrless}} t, \tag{13}$$

where t is a threshold level and $\mathbf{v}(\tau) \in \mathbb{C}^L$ is the vector

$$\mathbf{v}(\tau) := [v_1(\tau), \cdots, v_L(\tau)], \tag{14}$$

and $E(\tau)$ is the energy in the N_{slot} time slots,

$$E(\tau) = \sum_{k=1}^{N_{slot}} \int_{I_k} \|z(t-\tau)\|^2 dt. \tag{15}$$

Thus, in the analog beamforming case, the GLRT is simply performed with non-coherently adding the energy from the matched filter outputs for the L sub-signals.

IV. Simulation

We assess the performance of the directional correlation detector for both analog and digital beamforming under the parameters in Table I. The parameters are based on a realistic system design considerations described in detail in the full paper [14] For example, the parameters for the bandwidth, carrier frequency, and antenna patterns are based on the simulation study [5]. The PSS parameters T_{sig} and W_{sig} and T_{per} were selected to ensure the channel is roughly flat within each $T_{sig} \times W_{sig}$ PSS sub-signal time-frequency region based on typical time and frequency coherence bandwidths observed in [15]. The value T_{per} was then selected to keep a low (2%) total PSS overhead ($= T_{sig}/T_{per}$).

To compute the threshold level t in (7) and (13), we first computed a false alarm probability target with the formula

$$P_{FA} = \frac{R_{FA}}{N_{PSS}N_{dly}N_{FO}},$$

where R_{FA} is the maximum false alarm rate per search period and and N_{PSS}, N_{dly}, N_{FO} are the number of signal, delay and frequency offset hypotheses respectively – see the full paper [14]. The threshold level to meet the P_{FA} target was then estimated via Monte Carlo trials. We then measured the missed detection rate varying the SNR. For each SNR, we assumed that the beam directions in the arrays on both the TX and RX were randomly selected. For the analog beamforming case, both the TX and RX beams were randomly selected every PSS time slot. For the digital beamforming case, only the TX needs to select a random direction and that was selected independently in each sub-signal.

The results of the simulations are summarized in Fig. 2. The target SNR, shown is the figure is P/N_0W_{tot} where P is the total received signal power, W_{tot} the total available bandwidth and N_0 is the noise power density. As we can observe, there is a large gap in SNR between digital to analog beamforming to achieve an acceptable P_{MD} over the search period (≈ 18 dB for $P_{MD} = 0.01$). This gap is largely due to the fact that digital beamforming with the proposed eigenvector correlator can, in essence, determine the correct spatial direction over all the sub-signals, while analog beamforming can only look in one direction at a time. Since there are $N_{rx} = 16$ antennas at the UE in this simulation, determining the correct direction can lead to a gain of approximately 12 dB. Digital beamforming offers further gains since the TX can vary the beamforming direction in each sub-signal as opposed to each time slot.

To place this gap in context, it is useful to look at a typical edge rate minimum SNR requirement. Suppose that the UE should be able to connect whenever the SNR is sufficiently large for some target rate, R_{tgt}. If the system were operating at the Shannon capacity, it would achieve this rate at an SNR P/N_0 given by

$$R_{tgt} = \beta W_{tot}\log_2\left(1 + \frac{PG_{tx,max}G_{rx,max}}{N_0W_{tot}}\right),$$

where W_{tot} is the total system bandwidth, β is a bandwidth overhead fraction, and $G_{tx,max}$ and $G_{rx,max}$ are the maximum TX and RX antenna gains that could be achieved after the mobile has connected. For the SNR plotted on Fig. 2, we assume that P/N_0 is at the minimum value for R_{tgt}=10 Mbps, $W_{tot} = 1$ GHz and $\beta = (0.5)(0.8)$ to account for half-duplexing TDD constraints and 20% control overhead [5]. This minimum SNR is extremely low since the maximum gains in the antenna are very high: $G_{tx,max} = 64$ and $G_{rx,max} = 16$ for a combined total gain of 30 dBi. It is precisely this gain that makes the synchronization a challenge for mmW systems: high antenna gains imply that the link can meet minimum rate requirements at very low SNRs once the link is established and directions are discovered. But, in order to use the links in the first place, the mobiles need to be able to detect the base stations at these low SNRs before the directions are known. From Fig. 2, we see that with digital beamforming,

Parameter	Value
Total system bandwidth, W_{tot}	1 GHz
Number of sub-signals per PSS time slot, N_{sig}	4
Subsignal Duration, T_{sig}	100 μs
Subsignal Bandwidth, T_{sig}	2 MHz
Period between PSS transmissions, T_{per}	5 ms
PSS overhead	2%
Search period, N_{slot}	50 slots = 250 ms
Total false alarm rate per search period, R_{FA}	0.01
Number of PSS waveform hypotheses, N_{PSS}	3
Number of frequency offset hypotheses, N_{FO}	23
BS antenna	8×8 uniform linear array
UE antenna	4×4 uniform linear array
Carrier Frequency	28 GHz
PSS SNR, PT_{sig}/N_0	varied

TABLE I: Simulation Parameters

the system can reliably detect the signal at an SNR for the 10 Mbps rate target. But, with analog beamforming, the system needs a significantly larger SNR. Although, it is not plotted, increasing the search time, N_{slot} even by a factor of ten, did not sufficiently improve the analog beamforming performance.

Of course, digital beamforming comes with a high power consumption cost since the A/D power consumption scales linearly with the number of antennas. However, since power consumption also scales exponentially with the number of bits, fully digital front ends may be feasible with very low bit rates per antenna as proposed in [12], [13]. Using a linear white noise model for the quantizer [16], it is argued in the full paper that the effective SNR after quantization can be approximated as

$$\gamma = \frac{(1-\alpha)\gamma_0}{1-\alpha+\alpha\gamma_0},$$

where $\gamma_0 = P/(N_0 W_{sig} N_{sig})$ is the SNR with no quantization error, γ is the effective SNR with quantization error and α is the average relative error of the quantizer. It is shown that even with a uniform 2-bit quantizer per antenna, the gap between γ_0 and γ is less than 0.5 dB under our simulation assumptions. The loss is extremely small since the SNR is already very low at the target rate, so the quantization noise is small.

CONCLUSIONS

We have proposed and analyzed a simple directional cell search procedure where the base station periodically transmits synchronization signals in random directions to scan the angular space. GLRT detectors are derived for the mobile for both analog and digital beamforming. The GLRT detectors are shown to reduce to matched filters with the synchronization signal, with an added eigenvector search in the digital case to locate the optimal receive spatial signature. Simulations under realistic parameters indicate that digital beamforming offers dramatically better performance than analog beamforming, and may be necessary to meet reasonable cell edge rate targets. In addition, we have argued that increase in power consumption for fully digital front-ends can be compensated by using very low bit rates per antenna with minimal loss in performance. These results suggest that a fully digital front-end with low rate per antenna with an appropriate search algorithm may be a fundamentally better design choice for cell search than analog beamforming that most designs are pursuing. In a future work, we will evaluate how analog transmission using different subsets of the available antenna elements and selecting only a fraction of the received power improves the detection process.

REFERENCES

[1] F. Khan and Z. Pi, "An introduction to millimeter-wave mobile broadband systems," *IEEE Comm. Mag.*, vol. 49, no. 6, pp. 101 – 107, Jun. 2011.

[2] P. Pietraski, D. Britz, A. Roy, R. Pragada, and G. Charlton, "Millimeter wave and terahertz communications: Feasibility and challenges," *ZTE Communications*, vol. 10, no. 4, pp. 3–12, Dec. 2012.

[3] S. Rangan, T. S. Rappaport, and E. Erkip, "Millimeter-wave cellular wireless networks: Potentials and challenges," *Proceedings of the IEEE*, vol. 102, no. 3, pp. 366–385, March 2014.

[4] T. S. Rappaport, *Wireless Communications: Principles and Practice*, 2nd ed. Upper Saddle River, NJ: Prentice Hall, 2002.

[5] M. R. Akdeniz, Y. Liu, M. K. Samimi, S. Sun, S. Rangan, T. S. Rappaport, and E. Erkip, "Millimeter wave channel modeling and cellular capacity evaluation," http://arxiv.org/abs/1312.4921, Dec. 2013.

[6] 3GPP, "Evolved Universal Terrestrial Radio Access (E-UTRA) and Evolved Universal Terrestrial Radio Access Network (E-UTRAN); Overall description; Stage 2," TS 36.300 (release 10), 2010.

[7] K.-J. Koh and G. Rebeiz, "0.13-μm CMOS Phase Shifters for X-, Ku-, and K-Band Phased Arrays," *Solid-State Circuits, IEEE Journal of*, vol. 42, no. 11, pp. 2535–2546, Nov 2007.

[8] K.-J. Koh, J. May, and G. Rebeiz, "A millimeter-wave (40-45 GHz) 16-element phased-array transmitter in 0.18-μm SiGe BiCMOS technology," *Solid-State Circuits, IEEE Journal of*, vol. 44, no. 5, pp. 1498–1509, May 2009.

[9] X. Guan, H. Hashemi, and A. Hajimiri, "A fully integrated 24-GHz eight-element phased-array receiver in silicon," *IEEE J. Solid-State Circuts*, vol. 39, no. 12, pp. 2311–2320, Dec. 2004.

[10] A. Alkhateeb, O. E. Ayach, G. Leus, and J. Robert W. Heath, "Hybrid precoding for millimeter wave cellular systems with partial channel knowledge," in *Proc. Information Theory and Applications Workshop (ITA)*, Feb. 2013.

[11] H. L. Van Trees, *Detection, Estimation and Modulation Theory, Part I*. New York, NY: Wiley, 2001.

[12] H. Zhang, S. Venkateswaran, and U. Madhow, "Analog multitone with interference suppression: Relieving the ADC bottleneck for wideband 60 GHz systems," in *Proc. IEEE Globecom*, Nov. 2012.

[13] D. Ramasamy, S. Venkateswaran, and U. Madhow, "Compressive tracking with 1000-element arrays: A framework for multi-Gbps mm wave cellular downlinks," in *50th Annual Allerton Conference on Communication, Control, and Computing (Allerton)*, Oct 2012, pp. 690–697.

[14] C. N. Barati, S. A. Hosseini, S. Rangan, P. Liu, T. Korakis, S. S. Panwar, and T. S. Rappaport, "Directional cell search for millimeter wave cellular systems," arXiv preprint, 2014.

[15] Y. Azar, G. Wong, K. Wang, R. Mayzus, J. Schulz, H. Zhao, F. Gutierrez, D. Hwang, and T. Rappaport, "28 GHz propagation measurements for outdoor cellular communications using steerable beam antennas in New York City," in *IEEE International Conference on Communications (ICC)*, June 2013, pp. 5143–5147.

[16] A. Gersho and R. M. Gray, *Vector Quantization and Signal Compression*. Boston, MA: Kluwer Acad. Pub., 1992.